ELSEVIER

Contents lists available at ScienceDirect

NeuroImage

journal homepage: www.elsevier.com/locate/ynimg





Overlaps of fMRI activation patterns of the anxiety-emotional and the vestibular-sensory networks

M. Lotze ^{a,1,*}, K. Klepzig ^{a,1}, T. Stephan ^{b,c}, M. Domin ^a, T. Brandt ^{b,1}, M. Dieterich ^{b,c,d,1}

- a Functional Imaging, Institute of Diagnostic Radiology and Neuroradiology, University Medicine Greifswald, Walther-Rathenau-Str. 46, Greifswald, D-17475, Germany
- ^b German Center for Vertigo and Balance Disorders (DSGZ), LMU University Hospital, Munich, Germany
- Department of Neurology, LMU University Hospital, Munich, Germany
- d SyNergy Munich Cluster for Systems Neurology, Munich, Germany

ARTICLE INFO

Keywords: Vestibular cortex Galvanic vestibular stimulation Fear conditioning Emotional representation Trait anxiety fMRI

ABSTRACT

Clinical and meta-analytic imaging data suggest a considerable overlap between vestibular-sensory and anxiety-emotional processing networks. We therefore examined functional MRI activation using galvanic vestibular stimulation (GVS) and a fear conditioning paradigm in the same 28 healthy individuals. This study was to proof the effects of both stimulations in the same individual whereas our earlier meta-analytical analysis compared groups of participants who had received only one or the other stimulation. In the actual study we further assessed subjective experience (expectancy ratings, questionnaires) and autonomic arousal (skin conductance response; SCR). Activation patterns during vestibular stimulation confirmed previous findings showing highest fMRI-activation in the parieto-insular vestibular cortex. Fear conditioning activated the anterior insula, secondary somatosensory cortex (S2) and thalamus. A conjunction of fMRI-activation maps for both stimulation paradigms revealed bilateral anterior and posterior insula, dorsolateral prefrontal cortex and S2 as well as cerebellar hemisphere fMRI-activation. Regression analyses showed a high positive association of left anterior insular activation during the fear extinction period with trait anxiety. The vestibular intensity during GVS was positively associated with right ventro-lateral prefrontal cortex (PFC) fMRI-activation. This is compatible with the earlier hypothesized top-down regulation of vestibular perception which involves the PFC beneficial for suppression of unusual vestibular excitation or vertigo related to vestibular disorders.

1. Introduction

For most species survival in their environment relies on the multisensory input from vestibular, visual, auditory, somatosensory, and olfactory sensors the processing of which is organized in central networks. These sensory networks are interconnected and embedded in higher cortical neuronal ensembles of cognition, memory, and emotion (Brandt and Dieterich, 2019). All together form a complex structure distributed from brainstem to cortex to subserve recognition, spatial orientation, memory, emotion, social interaction, and sensorimotor control of avoidance and attraction (Dieterich and Brandt, 2018). The latter function, e. g, motor responses initiated by sensory input depend on such factors as the actual body position, spatial memory, environmental structures, attention, and task-dependent voluntary intention. With

respect to brain structure and function an overlap of sensory and cognitive networks can be expected to enable this behaviour. An example is the conspicuously linkage between a vestibular stimulation and the associated emotional responses such as joy on a carousel or the fear to fall on a moving platform.

There is clinical evidence that episodic vestibular disorders such as Meniere's attacks or vestibular migraine are accompanied by a threatening anxiety (Eckhardt-Henn et al., 2008; Lahmann et al., 2015). The severity of anxiety in vertigo and balance disorders (either "excess anxiety" or "less anxiety") depend on the functional integrity of the vestibular system (Brandt and Dieterich, 2019). This is supported by a survey on a total of 7083 dizzy patients showing that inadequate vestibular stimulation by episodic vertigo syndromes is associated with increased vertigo-related anxiety while bilateral vestibular loss of

E-mail address: martin.lotze@uni-greifswald.de (M. Lotze).

 $^{^{\}star}$ Corresponding author.

 $^{^{1}\,}$ These authors contributed equally to this work.

function is associated with less vertigo-related anxiety (Decker et al., 2019) despite the impaired balance regulation with a high risk of falls. This also applies to chronic central vestibular disorders (Padovan et al., 2023). The psychiatric comorbidity of anxiety disorders and depression among patients suffering from vestibular vertigo syndromes is well recognized (Best et al., 2009; Bigelow et al., 2016; Eckhardt-Henn et al., 2008; Lahmann et al., 2015).

On the other hand, vertigo and dizziness are also symptoms in disorders of depression or anxiety or in functional disorders such as phobic postural vertigo (Brandt, 1996) also termed persistent postural perceptual dizziness, PPPD (Dieterich et al., 2016; Staab et al., 2017). In panic attacks vertigo or dizziness are one of the characteristic symptoms.

In addition, those patients with high anxiety tend to develop chronification of intermittent vestibular disturbances (Staab, 2019) with the consequences of a restricted community mobility and participation (Dunlap et al., 2025).

In a first attempt we tried to demonstrate a potential overlap of the vestibular and fear systems with regard to their brain imaging representation maps. Brain activation patterns were compared in two fMRI meta-analyses, one on fear conditioning (Fullana et al., 2018) and the other on vestibular stimulation (Neumann et al., 2023). Common clusters of concordance of vestibular stimulation and fear conditioning were found in, e.g., the bilateral insular and ventrolateral prefrontal cortex, and secondary somatosensory cortex. However, the functional interpretation of these data was limited because the two meta-analyses had been performed on different cohorts of healthy participants (Neumann et al., 2023). Therefore, in the current study two well established experimental procedures addressing vestibular and fear processing (differential fear conditioning and galvanic vestibular stimulation; GVS) were performed in the MRI in the same group of participants. The inclusion of questionnaires on State-Trait Anxiety Inventory (STAI) and Vertigo Symptom Scale (VSS) was chosen to uncover differences in inter-individual susceptibilities to vestibular related anxiety. Beside BOLD response we also recorded subjective experience (expectancy ratings of unpleasant stimulation experiences during GVS) and autonomic arousal (as skin conductance response; SCR) to understand possible cross-network associations with neural processing, and also to control for successful implementation of the paradigms. Specific questions were related to the exact localization of the activations in the core structures of both networks. We hypothesized that brain activation during GVS and fear conditioning should overlap regarding relevant sites. Also, we expected that self-report measures, BOLD-magnitude and SCR might be associated.

One additional hypothesis was based on our earlier assumption that there is a top-down regulation of vestibular perception which involves the prefrontal cortex (PFC) to enable suppression of unusual and unwanted excessive vestibular excitation or vertigo related to vestibular disorders (Decker et al., 2019; Brandt and Dieterich, 2019). This view is also supported by a psychophysical study showing that electrical stimulation of the dorsolateral prefrontal cortex (DLPFC) modulates vestibular perception and nausea elicited in healthy participants during sinusoidal galvanic vestibular stimulation (McCarthy et al., 2023) and a fMRI study disclosing BOLD signal intensity patterns in the parieto-insular cortex and thalamus comparing both transcranial DLPFC stimulation with concurrent sinusoidal galvanic vestibular stimulation (McCarthy et al., 2025). The confirmation of an overlap between the two networks, the vestibular und the anxiety-emotional, shows the structural basis for a coupling of anxiety and vestibular information processing. This would explain why patients with bilateral vestibular loss reported less vertigo-related anxiety (Decker et al., 2019). The coupling is also compatible with the observation of increased anxiety during unusual intense bodily accelerations and in episodic vertigo forms with preserved vestibular function, such as vestibular migraine and functional dizziness (Brandt and Dieterich, 2020).

2. Methods

2.1. Participants

28 right-handed and healthy adult participants (17 female, mean age: 23.5 ± 4.2 years) took part in the study which had been provided ethical commitment by the Ethics Committee of the University Medicine Greifswald (BB 029/23). Participants were recruited via flyer at the University and were predominantly medical students (n=14). Exclusion criteria were mental and neurological illnesses but also experiences with psychotherapy at present or in the past. In addition, participants with contraindication for MRI were excluded. The whole experimental session took about 1:30 h. Participants were financially compensated.

2.2. Questionnaires

To assess self-reported tendencies of anxiety and vertigo participants completed the German version (Laux et al., 1981) of the State-Trait Anxiety Inventory (STAI) (Spielberger et al., 1970) and the German version (Gloor-Juzi et al., 2012) of the Vertigo Symptom Scale (VSS) (Yardley et al., 1992). Besides total scores also the vertigo subscale score of the VSS were computed. VSS data of one individual could not be considered for analyses due to 8 omitted items.

2.3. Paradigms

2.3.1. Galvanic vestibular stimulation

Galvanic vestibular stimulation with alternating currents at a frequency of 1 Hz (AC-GVS) was applied in a block design (Stephan et al., 2005). The stimulation currents were produced by a battery driven stimulator built in-house, that was located inside the Faraday cage of the MRI scanner and was controlled using fiber-optic signal transmission. The experimental procedure was controlled by a computer running Presentation software (Neurobehavioural Systems, Berkeley, CA, USA). Carbon electrodes were attached using ten-20 paste over both mastoid processes after careful skin preparation (local anesthetics with lidocaine gel, cleaning with abrasive paste and saltwater solution), and secured with a head bandage. After placing the participants on the scanner table, a test stimulation was performed to make them familiar with the effects of stimulation and to find a suitable individual current strength. In order to maximize the intensity of the vestibular stimulation and minimize somatosensory sensations, participants were asked to choose an amplitude that produced a distinct vestibular sensation and at the same time allowed a stimulation for the whole duration of the experiment. This individual current amplitude varied between 1.5 mA and 3.5 mA (mean 2.14 ± 0.48 mA). We applied 15 trials of -GVS each with a duration of 8 s and preceded by a resting period (22 s). After the experiment participants answered questions about their experiences during GVS such as feelings of induced movement and their intensities (Stephan et al., 2005). For 4 participants these ratings were incomplete.

2.3.2. Fear conditioning

We applied a differential fear conditioning paradigm with a partial gain of 75 % that produces particularly strong effects in extinction (Lonsdorf et al., 2017). As an aversive unconditioned stimulus (UCS), a pneumatic tactile stimulation had been applied to the left index finger upper segment (nail fold) by using a small plastic cylinder driven by an Impact Stimulator (Labortechnik Franken, Germany; Release 1.0.0.34; European Standard EN 60,601-1 Medical Electrical Devices). This method is a reliable alternative to electrical stimulation as it has been successfully used by our research group to investigate extinction learning (Lindner et al., 2015; Wendt et al., 2017) and emotion processing (Holtz et al., 2012; Lotze et al., 2007; Wendt et al., 2008). Prior to the experiment the intensity of the pneumatic tactile stimulation (UCS) was individually adjusted to a "clearly unpleasant, but not painful" level (mean intensity 4.4 ± 0.9 g/s). During acquisition two

geometric shapes (blue square, orange circle) were presented 12 times each while one of the geometric shapes (CS+) was paired with the UCS (applied 6.5 s after onset of the CS+) in 75 % of the trials (9 times). The other geometric shape (CS-) was never accompanied by the UCS. During the extinction phase, both geometric shapes (CS+, CS-) were presented again 12 times each, without application of the UCS. Before each presentation of a geometric shape participants were asked to rate the probability (expectancy in %) of the occurrence of an UCS using a LUMItouch key pad (Photon Control Inc., Burnaby, Canada) and a visually presented scale with 10 percent increments. To accommodate to the rating procedure a training session was realized prior to the experiment. All visual stimuli were presented via LCD screen (NordicNeuroLab, Bergen, Norway) placed behind the scanner and a mirror mounted to the MR head coil. Participants were randomly assigned to one of two presentation orders (UCS either paired with circle or with square). Presentation software was used for stimulus presentation and recording of UCS expectancy ratings. Mean UCS expectancy ratings were calculated considering the first and the last 6 trials respectively for acquisition and extinction for both stimuli (CS+, CS-). Then, differential mean expectancy ratings (i.e., (CS+) - (CS-)) were computed (Lonsdorf et al., 2017). Also, differential mean values were computed respectively across all acquisition and extinction trials. Expectancy ratings of two participants were not available due to recording problems (n = 1) and misunderstanding of instructions (n = 1).

2.4. Measurement and preprocessing of skin conductance response (SCR)

Skin conductance has been recorded during both experimental procedures using two Ag/AgCl electrodes with a diameter of 4 mm filled with an electrode cream and placed adjacently on the hypothenar eminence of the left hand. The sampling rate was set at 5000 Hz. Electrodes were connected via a GSR-MR module and BrainAmpExG MR amplifier to a computer running BrainVision recording software (Brain Products, Gilching, Germany). Skin conductance data were downsampled to 10 Hz and exported to a txt-file using BrainVision Analyzer 2.0 (Brain Products). Analyses were then realized with Ledalab software package (Benedek and Kaernbach, 2010) in Matlab which separates the signal into a tonic and phasic component through a deconvolution approach. SCR was scored as the average phasic driver in μS which constitutes the most adequate measure of phasic activity (Benedek and Kaernbach, 2010). For the examination of vestibular stimulation SCR was assessed during GVS (0.9-8.0 s after GVS onset) and during rest (6.9–14.0 s after rest onset). The rationale for the latest possible analysis window during the resting period was to collect resting-state SCR and, hence, to rule out possible after-effects of the galvanic stimulation.

SCR data (GVS) was not available for one participant due to technical malfunction. For the fear conditioning paradigm SCR was assessed during the presentation of the visual stimuli (0.9–7.0 s after onset). Analysis windows starting 0.9 s after stimulus onset and covering the whole stimulus duration were chosen in accordance with latency and rise time characteristics of the SCR signal (Giannakakis et al., 2022; Sjouwerman and Lonsdorf, 2019).

A logarithmic transformation of the SCR (Venables and Christie, 1980) followed by a range correction ($x_{corrected} = x / x_{max}$) (Lykken and Venables, 1971) was carried out to normalize the distribution and to reduce inter-individual variability not related to the task.

Mean SCR across all GVS trials was computed. For fear conditioning mean differential SCR values were calculated as described for UCS expectancy ratings. For both experiments SCR means were computed respectively with raw and logarithmized/range-corrected values.

2.5. Statistical analysis of ratings and SCR

To examine SCR during GVS a repeated measures (rm) ANOVA with *Condition* (GVS, rest) and *Trial* (1–15) as within-subjects variables was conducted. Differential UCS expectancy ratings and differential SCR

were examined with rmANOVAs with *Phase* (acquisition, extinction) and *Time* (early, late) as within-subjects factors. Examining SCR with rmANOVAs was realized respectively with raw and logarithmized/range-corrected values. To examine the impact of self-reported anxiety and vertigo tendencies on the course of raw SCR groups with low and high scores were created using median splits of the questionnaire data (STAI scores, VSS total score). Then, rmANOVAs were computed as described above with *Score* (high, low) as additional between-subjects factor.

Spearman's rank correlations were applied to examine associations among questionnaire data, ratings and raw SCR means. Alpha was set at 0.05. Analyses were conducted using SPSS version 22 (IBM Corporation, Armonk, NY, USA). Plots were created with R (v4.1.2). Fig. 1 shows the experimental set-up and descriptions of the course of stimuli.

2.6. MR-imaging

Imaging data was collected at a 3T MRI-scanner (Vida, Siemens, Erlangen, Germany) with a 64-channel head coil. Functional imaging was performed with a multiband EPI sequence (CMRR; Center for Magnetic Resonance Research, Department of Radiology, University of Minnesota) of 60 transversal slices (multi-band acceleration factor of 5). The in-plane resolution was $2.5 \times 2.5 \text{ mm}^2$ and the slice thickness was 2.5 mm. The field of view was $220 \times 220 \text{ mm}^2$, corresponding to an acquisition matrix of 88×88 . The repetition time was 1 s, the echo time was 37 ms, and the flip angle was 52° For susceptibility-induced distortions spin-echo field maps were acquired in the same phase-encoding direction as the bold time series and in the opposite direction (anterior->posterior vs. posterior->anterior), geometry parameters similar to the bold time series, TR=6.9 s, TE=76.8 ms. Structural imaging was conducted using a sagittal T1-weighted 3D MPRAGE with 176 slices, and a spatial resolution of $1 \times 1 \times 1$ mm³. The field of view was 250×250 mm², corresponding to an acquisition matrix of 256 \times 256. The repetition time was 1690 ms, the echo time was 2.53 ms, the total acquisition time was 3:50 min, and the flip angle was 9° For the T1-weighted images, GRAPPA with a PAT factor of 2 was used. We used a rubber foam head restraint to avoid head movements.

2.7. fMRI preprocessing and statistical analysis

MRI data were visually inspected for imaging artifacts. FSL's topup (Andersson et al., 2003) was used to calculate a displacement field from the spin-echo field maps in order to correct for susceptibility-induced distortions. Motion correction and normalization to Montreal Neurological Institute (MNI) 152 non-linear template was performed using the Advanced Normalization Tools (ANTs, v2.3.5.dev212-g44225) (Avants et al., 2011). After motion correction the resulting motion parameters were examined regarding excessive motion, using a volume-to-volume threshold of 2 mm translation as well as 2 degrees of rotation in every direction. As the participants were firmly instructed regarding head motion as well as spatial and temporal resolution were high, any exclusion of data sets was not necessary. A concatenated transformation was calculated from these registration step and applied in a single resampling step to the BOLD time series. Gaussian smoothing of 8 mm FWHM (full width at half maximum) was applied to improve signal-to-noise ratio and to comply with the requirements of the Gaussian Random field theory. Six motion parameters were extracted from the linear registration of the motion correction for later inclusion into the statistical model.

Statistical parametric mapping was performed with SPM12 (Well-come Department of Neuroscience, London, UK) and Matlab version R2021b (MathWorks Inc, Natick, MA, USA). First-level analyses were performed with the general linear model (GLM), using a canonical hemodynamic response function (HRF) and to correct for low-frequency components, a high-pass filter with a cut-off of 128 s was used. Onsets and durations of the experimental conditions were extracted from log

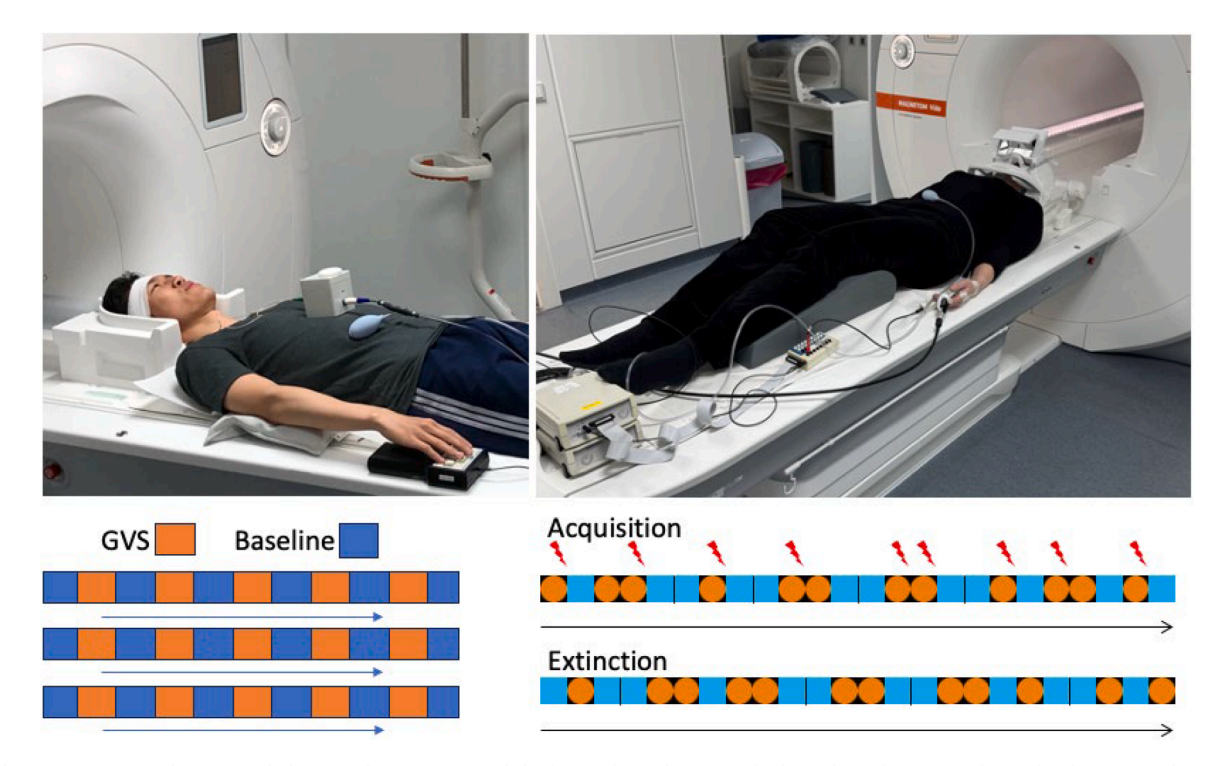


Fig. 1. The apparatus for galvanic vestibular stimulation (GVS) and the key pad are shown on the left. The right picture shows the devices for skin conductance response (SCR)-measurement and UCS stimulation. The bottom shows the time course of the GVS examination (left) and the fear conditioning paradigm (right). The occurrence of an unconditioned stimulus (UCS) is indicated by a flash.

files generated by Presentation. For the fear conditioning paradigm each of the four conditions of the fear conditioning paradigm (acquisition, extinction; CS+, CS-), the respective regressors were included as regressors of interest, but those of all the other trials (e.g., button presses) were included as regressors of no interest. For the vestibular stimulation condition onset and duration of GVS were inserted as condition. Any remaining time series data comprised the baseline. The residual effects of head motions were corrected for by including the six estimated motion parameters for each participant as regressors of no interest.

For the second-level analyses, contrast images for comparisons of interest (CS+ acquisition, CS+ extinction; CS- acquisition, CSextinction) were initially computed on a single-subject level. In the next step, the individual images of the main contrast of interest (CS+ minus CS- acquisition) were regressed against the UCS expectancy rating (how probable is it to receive a tactile stimulation?) and changes in SCR, using second-level regressions. Second-level results were corrected for multiple comparisons, using cluster-level family wise error (FWE) correction on a whole brain level (p_{FWE}<0.05). In addition, a region of interest (ROI) approach was performed for anatomical masks known to be activated during paradigms form earlier studies (for fear conditioning: (Wendt et al., 2017); for vestibular stimulation: (zu Eulenburg et al., 2012). These ROIs were also used for regression analyses between fMRI-amplitude during CS+ > CS- (Acquisition and Extinction separately) and vestibular stimulation in association with SCR-amplitude, ratings and STAI scores (trait and state). The ROIs comprised: Insula (anterior/posterior; Neuromorphometric atlas), S2 (Anatomy atlas), cerebellum (AAL), for prefrontal areas: the anterior cingulate cortex (ACC), the frontal eye field (FEF; coordinates with 1 cm spheres from meta-analysis (left: -28, -6, 54; right: 30, -6, 50) (Bedini et al., 2023), dorsolateral prefrontal cortex (DLPFC; AAL), Broca-area and analogon (BA 44/45; AAL), hypothalamus (Anatomy Atlas), hippocampus (Anatomy Atlas; right posterior hippocampal grey matter volume is associated with experience in slackline training in ballet/ice dancing or slacklining (Hüfner et al., 2011), amygdala (Anatomy Atlas), and thalamus (AAL). Associations with self-reports (STAI, VSS: vestibular strength, scoring of aversiveness of UCS) were calculated based on prior observations (e.g., anxiety: Harrison et al., 2015). Associations of logarithmized/range-corrected SCR values with fMRI-activation ROIS were calculated for the following ROIs based on prior observations (Anders et al., 2004): OFC, insula, thalamus. Linear regression in SPM12 was calculated for felt intensity of perceived movements and fMRI-activation during GVS. For fear conditioning association analyses were conducted for differential UCS expectancy ratings (CS+ minus CS-) during acquisition and extinction and STAI scores.

3. Results

3.1. Questionnaires

Mean scores were 32.0 \pm 5.5 (STAI state), 34.6 \pm 9.4 (STAI trait) and 13.9 \pm 8.5 (VSS). STAI scores above clinical thresholds were reached by 3 (state) and 5 (trait) participants. For the VSS vertigo subscale (group mean: 2.9 \pm 2.1) a clinical cut-off (4.5) was proposed (Gloor-Juzi et al., 2012) which was reached by 6 participants. The VSS correlated positively with both STAI scores (state: r=0.387, p=.046; trait: r=0.440, p=.022). Questionnaire data correlated in parts significantly with chosen UCS intensity (STAI state: r=-0.385, p=.043; VSS: r=-0.709, p<.001) but not with GVS intensity (ps>0.1).

3.2. Ratings and self-reports

All participants noticed the GVS while sixteen participants reported the experience of movement with an average intensity of 6.7 ± 1.7 on a scale from 0 to 10 (see left panel of Fig. 2 for the number of further reported experiences). The individual number of further reported experiences during GVS correlated significantly with the STAI state score (r = 0.442, p = .018) but not with STAI trait, VSS and GVS intensity (ps > 0.1). During the conditioning paradigm differential expectancy ratings (i.e., (CS+) - (CS-)) were higher for acquisition than for extinction (F(1,25) = 27.238, p < .001). Differences between CS+ and CS- were

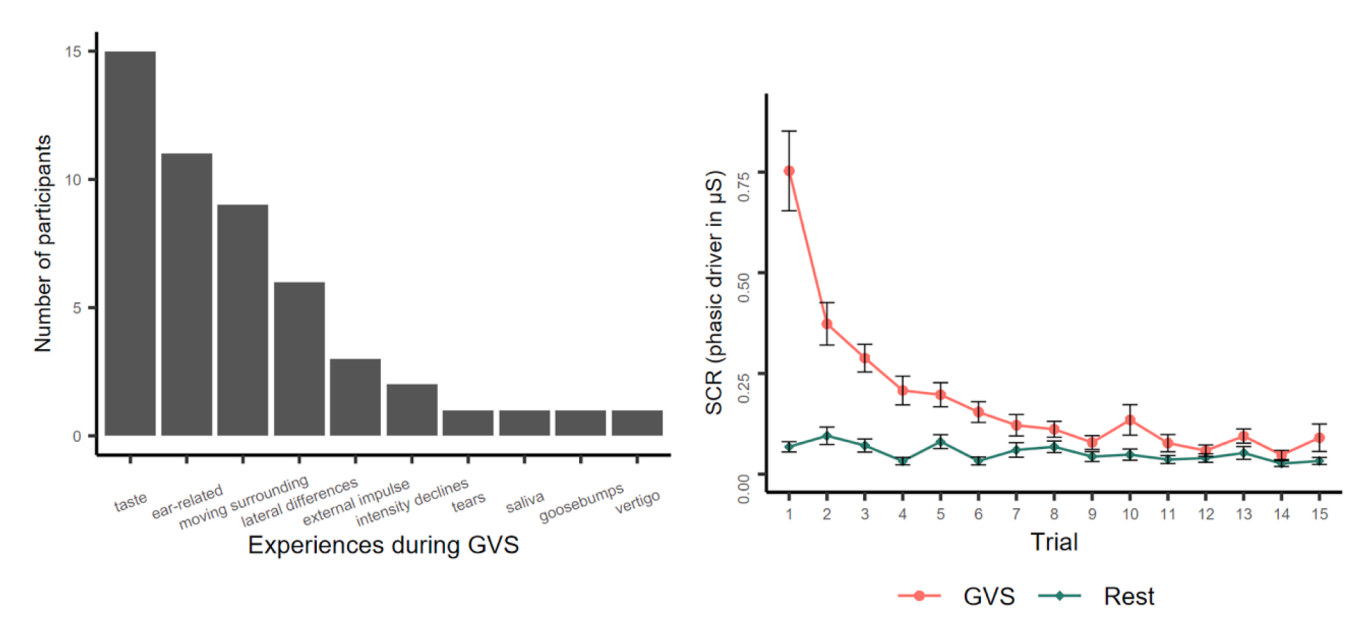


Fig. 2. Frequency of reported experiences during GVS (left panel) and mean raw SCR during GVS and rest (right panel). SCR = Skin conductance response, GVS = galvanic vestibular stimulation. Error bars represent standard errors of means.

highest during late acquisition and lowest during late extinction which was reflected by a significant interaction between *Phase* and *Time* (F (1,25) = 222.783, p < .001) (see top row of Fig. 3). Differential expectancy ratings correlated negatively with the VSS score (acquisition: r = -0.386, p = .057; extinction: r = -0.412, p = .041). No significant correlations could be found with STAI scores, number of experiences during GVS and UCS intensity.

3.3. Skin conductance response (SCR)

SCR during GVS was higher than SCR during rest (F(1,26) = 43.692, p < .001) while a habituation over time was noticeable and reflected by a significant interaction between Condition and Trial (F(14,364) =30.512, p < .001). Paired t tests with Bonferroni corrections showed that SCR towards GVS was increased primarily during the first 6 trials (ps < 0.05) (see right panel of Fig. 2). Mean SCR towards GVS was significantly correlated with the number of reported experiences during GVS (r = 0.395, p = .042) but not with GVS intensity and questionnaire data (ps > 0.1). During the conditioning paradigm differential SCR (i.e., (CS+)-(CS-)) was larger for acquisition than for extinction (F(1,27) = 8.600, p= .007). Differences between CS+ and CS- were most prominent during early acquisition and decreased over time resulting in a significant interaction between *Phase* and *Time* (F(1,27) = 10.484, p = .003) (see bottom row of Fig. 3). Differential SCR during acquisition correlated significantly with differential expectancy ratings during extinction (r =0.633, p = .001) while no other correlations of SCR could be found (rs >0.1). Using logarithmic transformation and range-correction of SCR data did not change outcomes and yielded rmANOVA results comparable to those computed from raw SCR data (see above). For the GVS paradigm a significant interaction between STAI state Score, Time and Condition was found indicating a larger initial SCR towards GVS in those with high STAI state scores compared to those with low STAI state scores (F (14,728) = 2.408, p = .003). For the conditioning paradigm a significant interaction between VSS total Score, Phase and Time was found which reflects a stronger decrease in differential SCR during late acquisition in those with low VSS scores compared to those with high VSS scores (F(1,52) =4.302, p = .049). Significant between-subjects factors or further significant three-way interactions between main factors could not be observed.

Error bars represent standard errors of means. UCS = Unconditioned stimulus, CS+= Geometric shape paired with UCS during acquisition,

CS- = Geometric shape never paired with UCS, acq. = acquisition, ext. = extinction, SCR = skin conductance response.

3.4. fMRI - effects

Main effects are in depicted in Supplemental Fig. ${\bf 1}$ and plotted in Supplemental Table 1.

Overall, our group results are completely in line with prior studies on fMRI-representations for both stimulation paradigms. In detail, GVS showed fMRI activation in bilateral anterior and posterior insula, bilateral secondary somatosensory cortex (S2), bilateral primary auditory cortex (A1), bilateral cingulate cortex (CC), and bilateral dorsolateral prefrontal cortex (dIPFC) reaching into right dorsal premotor cortex (dPMC; Supplemental Table 1A). For fear conditioning CS+ > CS-showed fMRI-activation in bilateral anterior insula, bilateral S2, left dIPFC and bilateral thalamus (Supplemental Table 1B).

When testing overlaps between representation sites for both paradigms we calculated a conjunction analysis revealing bilateral anterior and posterior insula, S2, Broca-area/Broca-analogon and left cerebellar hemisphere (see Fig. 4 and Table 1).

When calculating differences between both stimulation paradigms GVS minus fear conditioning revealed fMRI-activation in bilateral occipital lobe, left PFC, right lingual gyrus, right S2, bilateral cerebellar hemispheres, and ACC (Fig. 5, Table 2). In contrast, fear conditioning minus GVS revealed fMRI-activation in left anterior insula, left S2, bilateral thalamus and bilateral PAG.

Fig. 5 shows differences between both paradigms.

3.5. fMRI- regression analyses

When testing associations between ratings (GVS: experienced vestibular effect strength; fear conditioning; acquisition or extinction phase: shock expectancy, anxiety ratings) we found the following effects. The intensity of experience of dizziness during vestibular stimulation was associated with right vlPFC/orbitofrontal fMRI-activation (r=0.70; p<.001; ROI-correction for OFC with t=4.63; p_{FWE_ROI}=0.048; coordinates: 30, 39, -18; see Fig. 6, left). During extinction participants with high trait anxiety showed high anterior insula activation (left: t=5.23; pFWE insula=0.004; coordinates: -36, -3, 9, p_{FWE_whole_brain} 0.044; right: t=5.04; pFWE insula=0.007; coordinates: 39, -18, 0; Fig. 6, middle). Those who did show high shock expectancy during the

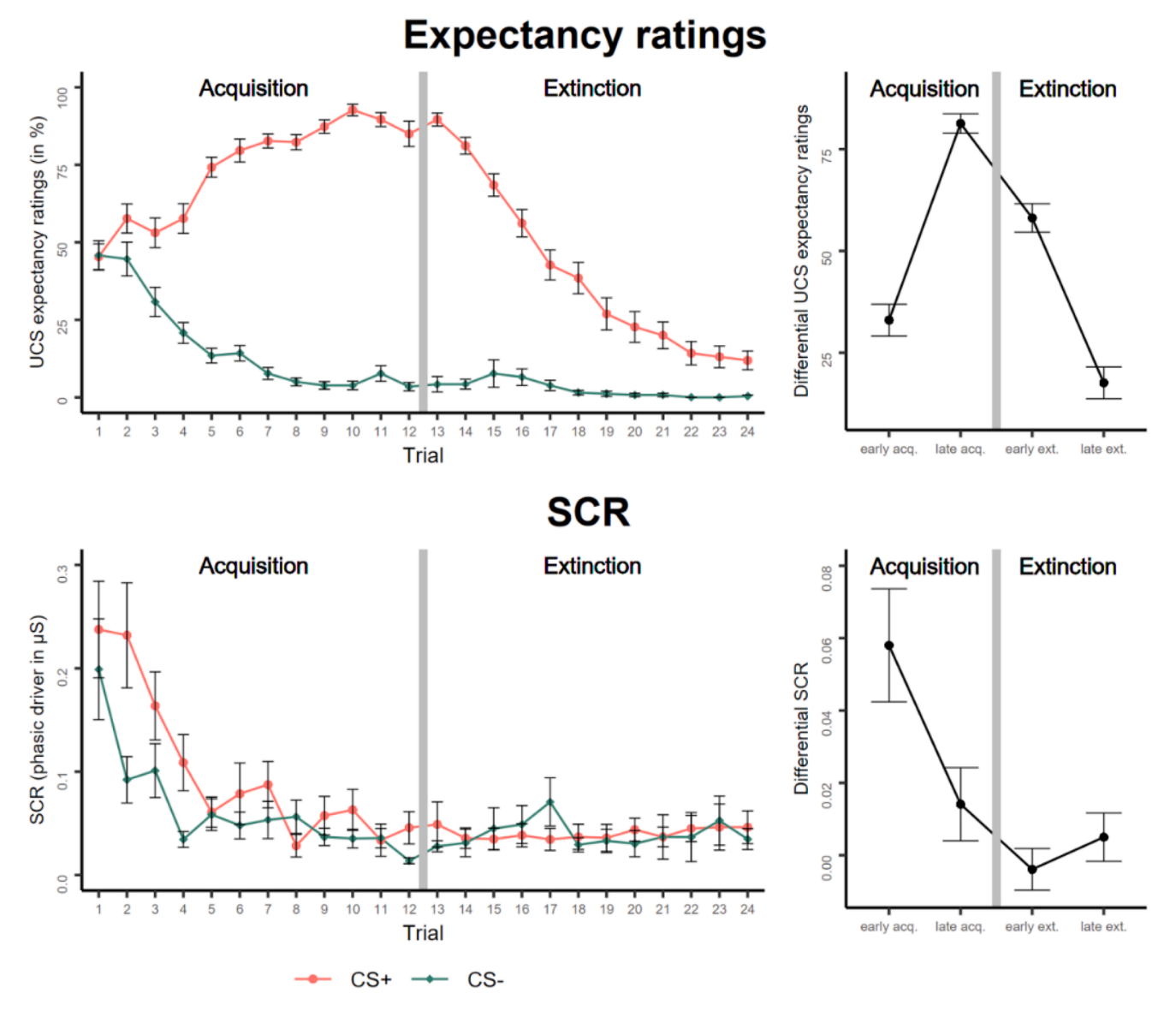


Fig. 3. Top: Mean UCS expectancy ratings trial-wise (left panel) and mean differential UCS expectancy ratings ((CS+) - (CS-)) (right panel). Bottom: Mean raw SCR trial-wise (left panel) and mean raw differential SCR (right panel).

extinction phase of fear conditioning additionally showed low right sided hippocampal fMRI-activation (r=-0.62; p<.005; t=3.92; pFWE_ROI=0.045; coordinates: 36, -24, -15; Fig. 6, right) indicating an association between low cognitive memory recruitment and higher fear of being shocked during the shock-free extinction phase.

4. Discussion

In the present study we examined overlaps between neural activation patterns during anxiety and vestibular sensations in the same healthy individuals. For that purpose, we conducted two well established procedures (GVS and fear conditioning) in order to experimentally induce these states, while recording subjective perceptions, BOLD responses, and autonomic arousal (as SCR). Additionally, state of the art self-report questionnaires targeting anxiety and vertigo were applied. Although a clinical cut-off score of the vertigo subscale was reached by 6 participants, the highest individual score (7) was below lower quartiles of clinical samples (Gloor-Juzi et al., 2012), hence indicating only minor vertigo symptoms, if any.

Self-reports and SCR

Increased SCR during GVS reflected a reliable vestibular stimulation

in the participants which is further supported by a positive association with the number of reported sensations. Hence, in accordance with (Gavgani et al., 2017) measuring SCR offers a handy way to objectively assess GVS induced states and vestibular sensations in general. Interestingly, the majority of participants reported taste-related sensations during GVS which might be due to involuntary head movements inside the scanner (Cavin et al., 2007). During the differential fear conditioning paradigm, UCS expectancy ratings and SCR were comparable to data of a recent work confirming a successful implementation of the paradigm (Dibbets and Evers, 2017). A negative correlation of STAI and VSS scores with chosen UCS intensity is in line with Tang and Gibson (2005) who found that higher state anxiety is associated with higher sensitivity to pain.

Self-reported anxiety correlated positively with both self-reported vertigo (VSS) and the number of experimentally induced vestibular sensations representing overlaps of the two perceptional entities. This is in line with a study by Saman et al. (2016) who found in vestibular schwannoma patients with unilateral deafferentation a correlation of STAI anxiety and subjective instability during caloric vestibular stimulation. Our finding of a negative correlation between the capability to differentiate between threat and safety signals (i.e., differential UCS

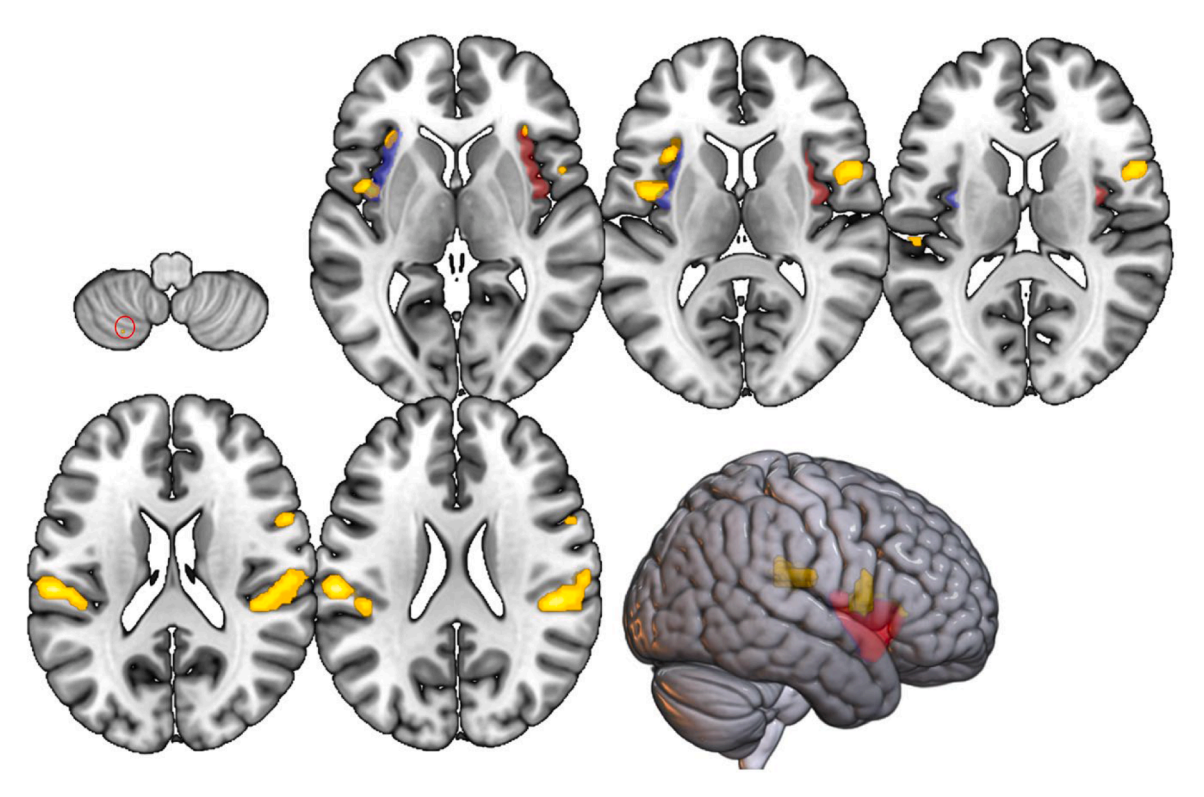


Fig. 4. For the conjunction between both paradigms (for fear conditioning only for the acquisition phase) left posterior cerebellar hemisphere (circle indicating location), bilateral anterior and posterior insula, bilateral S2 and Broca-area / Broca-analogon showed significant fMRI-activation (color coded in yellow-orange). Left anterior insula is indicated with transparent blue, right anterior insula with transparent red. Z-values for slicing; top row: –56, 3, 10, 14; bottom row: 20, 23 and render brain right hemisphere.

Table 1 Conjunction analysis.

ter size

Whole brain FWE significance: ** $p \le 0.05$; ROI-FWE significance: *.

expectancy) and self-reported vertigo is compatible with this view because bodily symptoms related to vertigo and assessed by the VSS are typically reported during fear and anxiety (Yardley et al., 1992), also discussed by Coelho and Balaban (2015). In turn, increased anxiety could hamper differential fear conditioning by stimulus generalization during acquisition as recently shown (Dibbets and Evers, 2017).

Although we did not find significant correlations of SCR with questionnaire scores, analyses using median splits showed that participants with more pronounced state anxiety had at least a higher initial SCR towards GVS than those with lower state anxiety which could again underline the association between anxiety and vertigo given that SCR is a reliable indicator of vertigo. Similarly, in a recent work on fear of heights and vertigo induction autonomic arousal was especially pronounced in those participants with increased fear (Bzdúšková et al., 2022). Hence, reducing anxiety might lower the intensity of experienced vertigo when exposed to corresponding stimulations which could be of therapeutic relevance in high-risk cohorts. Furthermore, a higher tendency towards vertigo was associated with a slower decline in

differential SCR during late acquisition, which might be due to delayed SCR habituation. Actually, a delay in SCR habituation has been shown for anxious participants (Raskin, 1975) while anxiety was also found to be positively correlated with SCR towards CS+ during acquisition (Indovina et al., 2011). Our data suggests that participants with a more pronounced vertigo might show a similar delay in SCR habituation.

Since our examination started with the GVS paradigm an after-effect of vestibular stimulation on fear conditioning might be thinkable. Therefore, UCS expectancy ratings and SCR data were compared with those of ten healthy participants in a similar age range (valid rating data n=8, valid SCR n=9) who did not receive GVS using rmANOVAs with an additional between-subjects factor (GVS, no GVS). As no differences could be found (ps > 0.05) we concluded that effects of GVS on variables of fear conditioning are less likely and that shared functional activation patterns during both paradigms are independent of each other.

4.1. Comparison of functional MRI activations during both paradigms

We identified overlaps and differences in representation sites between both paradigms. In a conjunction analysis both showed fMRI-activation in bilateral anterior and posterior insula, bilateral S2 and left inferior/posterior cerebellar hemisphere. Bilateral S2 and insula fMRI-activation had been already identified as common representations for different stimulation methods for vestibular stimulation ((Dieterich et al., 2003; Dieterich and Brandt, 2008); meta-analyses: (Neumann et al., 2023; zu Eulenburg et al., 2012)). Cerebellar activation was centered in Larsell's lobule VIIIA which is part of a second motor cortical–cerebellar loop (Kelly and Strick, 2003) showing a convergent representation of movement and sensory information from the whole body. A posterior cerebellar contribution for fear conditioning had been described before (Couto-Ovejero et al., 2023; Medina et al., 2002). In an electrophysiological study on rodents a close interaction between the cerebellum and emotional processes was found via a subset of zona

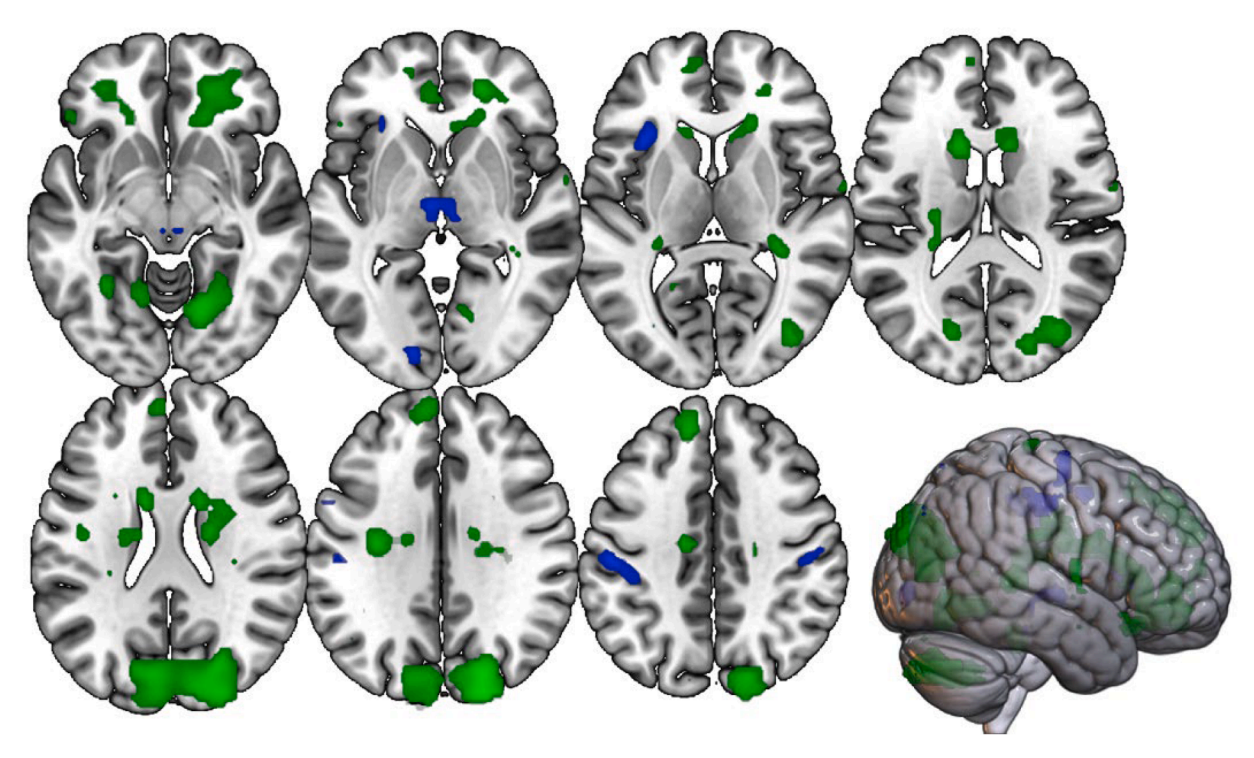


Fig. 5. GVS (green) showed higher fMRI-activation in bilateral superior occipital gyrus, left orbital gyrus, right lingual gyrus, right S2, bilateral cerebellar hemispheres and ACC. Fear conditioning (CS+ minus CS- during acquisition; blue) showed higher fMRI-activation in left anterior insula, FEF and S2, bilateral thalamus and bilateral PAG. Slice position: z = -8, -2, 3, 17, 23, 31, 39, right hemisphere of the rendered brain.

 Table 2

 Plotted differences between both conditions.

A) Vestibular stimulation minus fear conditioning (acquisition phase)				
Region	coordinates	t-value	Cluster size	
Right superior occipital gyrus	21, -81, 30	6.37**	101	
Left superior occipital gyrus	-9, -81, 24	5.19**	4	
vlPFC; Lateral orbital gyrus left	-33, 45, -12	5.84**	10	
Lingual gyrus right	15, -66, -6	5.15**	5	
S2 right	33, -21, 27	4.09*	17	
Cerebellar hemispheres;				
right:	36, -75, -42;	4.50*	245	
left:	-18, -33, -27	4.45*	24	
ACC	-6, 42, 0	3.77*	17	

Region	Coordinates	t-value	Cluster size
Ant insula left	-30, 27, 3	4.08*	13
S2 left	-51, -24, 39	4.51*	28
Thalamus left	-6, -15, -0	4.37*	17
Thalamus right	6, -24, -3	4.05*	13
PAG left	-3, -27, -6	3.52*	1
PAG right	-3, -27, -6	3.38*	2

^{**} p<.05 FWE whole brain corrected.

incerta neurons (through long-range glutamatergic and GABAergic transmissions (Zhao et al., 2025)). This prompted the authors to suggest the cerebellum for stimulation treatments in anxiety disorders.

Overall, the cortical activation overlaps between vestibular stimulation and fear conditioning showed quite consistent results when compared to those obtained by the recent meta-analysis (Neumann et al., 2023). However, there were also some differences to the meta-nalytic approach probably because of methodological issues such as different group sizes allowing for detecting smaller effect sizes in the metanalysis. For instance, anterior cingulate was not significantly activated during fear conditioning in our study but was active during GVS.

This area had been discussed to be related to avoidance behavior interacting with motor areas for flight reaction (Schlund et al., 2016). In addition, the latter meta-analytic approach did not allow for direct comparisons between conditions.

Increased fMRI-activation during GVS, when subtracted with those during fear conditioning (acquisition phase), was seen in areas which have been functionally related to visual processing (bilateral superior occipital areas and right lingual gyrus), the ventro-lateral PFC (cognitive and emotional processing), right S2 (as part of the parieto-insular vestibular network with the posterior insula and OP2, as the core region (Eickhoff et al., 2006; Lopez et al., 2012), the cerebellar hemispheres and the anterior cingulate cortex (ACC). Right S2 showed increased fMRI-activation during GVS according to observations in our previous meta-analysis (Neumann et al., 2023). Other non-ROI related findings for the analysis "GVS minus fear conditioning" revealed representation sites mostly in the DLPFC and the occipital lobe. The DLPFC was part of both networks in our meta-analysis (Neumann et al., 2023), i.e., is involved in emotional/anxiety and vestibular processing. Since the vestibular core region in the posterior insula receives input from the DLPFC, McCarthy et al. (2023) hypothesized a top-down control of vestibular inputs. They found a suppression of the vestibular sensations elicited by simultaneous GVS and transcranial sinusoidal electrical stimulations of the DLPFC. The same paradigm of simultaneous stimulation was performed in an fMRI study that showed an inhibitory function on vestibular processing exerted by the DLPFC (McCarthy et al., 2025). In our earlier meta-analytical study we proposed a similar concept of a down-regulation of the fear network by acute vestibular disorders or unfamiliar vestibular stimulations making unpleasant perceived body accelerations and nausea less distressing (Neumann et al., 2023). This concept was based on the differential effects of galvanic stimulation (activation) and fear conditioning (deactivation) of the posterior insula. Further, it fits the clinical observation that patients with bilateral vestibular loss suffer from less vertigo related anxiety (Brandt and Dieterich, 2020; Decker et al., 2019). Indeed, this concept is in line with a pilot study on patients with functional dizziness in whom

^{*} p<.05 FWE ROI corrected.

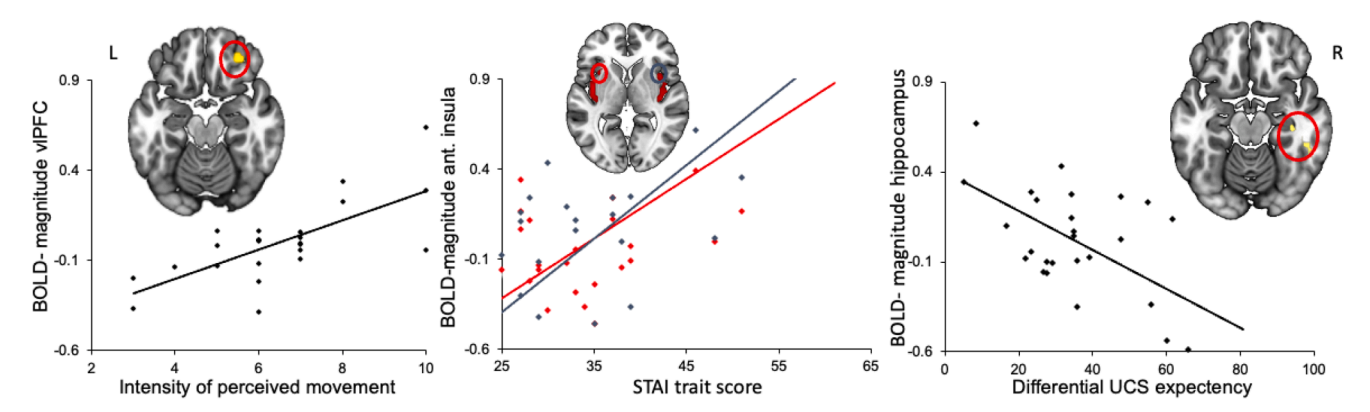


Fig. 6. Plots show correlations between intensity of perceived body sway during GVS and fMRI-activation in right vLPFC (left; axial slice position z=-18), between left (red) and right (blue) anterior insula fMRI-activation during the fear conditioning extinction phase and STAI trait score (middle; axial slice position z=3) and between hippocampus activation and differential UCS-expectancy ratings during the fear conditioning extinction phase (right; axial slice position z=-17).

repetitive electrical stimulation of the left DLPFC led to a considerable reduction of dizziness and subjective postural instability (Palm et al., 2019). Electrical stimulation of the DLPFC furthermore attenuated the skin-sympathetic nerve activity (Wong et al., 2023) and modulated muscle sympathetic nerve activity (McCarthy et al., 2023). Our data on SCR during GVS are in agreement with these studies.

For the contrast "fear conditioning minus GVS" the present analysis disclosed increased fMRI effects for fear conditioning in the left anterior insula, left S2, bilateral thalamus, bilateral periaqueductal gray (PAG) and left FEF. These effects are characteristic for fear conditioning results reported in both meta-analytic (Fullana et al., 2018) and single group publications (e.g. of our group: (Lindner et al., 2015; Wendt et al., 2017)) and seem to be centered on the arousal dimension of fear conditioning (e.g. thalamus: (Anders et al., 2004), PAG: (Wendt et al., 2017)).

4.2. GVS induced perception of body sway and fMRI activation

VLPFC activation was positively associated with the intensity of induced perceived movements scored after GVS. Adjacent regions (more lateral: BA47) have been reported to be associated with the valence dimension of emotional intensity in different paradigms (prosody: (Wildgruber et al., 2006); expressive gestures: (Lotze et al., 2006)). Therefore, we interpret the finding of OFC fMRI-activation in relation to rated perceived movements as emotional appraisal of the intensity of perception.

4.3. Associations of fear and fMRI activation

Regression analyses testing associations between fMRI-amplitude and questionnaires (perceived intensity of induced movements, VSS, STAI) showed a considerable positive relation of trait anxiety and bilateral anterior insula activation during the fear extinction phase. Our finding is in line with those of Harrison and colleagues (Harrison et al., 2015) reporting anterior insula activation in association to perceived anxiety in a fear conditioning experiment. Differing patterns of anterior insular activity between depression subtypes clarify the complex interaction between anxiety and depression, emphasizing the insula's crucial role in processing diverse emotional stimuli (Ren et al., 2025). In addition, an absent differential conditioning effect during extinction had been reported for patients with panic disorders (Lueken et al., 2015) but might be also critical in patients with chronic pain (Flor, 2012). fMRI-activation in the right hippocampus was negatively related to differential UCS expectancy ratings during the extinction phase of the current study. The hippocampus is important for learning and therefore also crucially involved in fear conditioning. Adequate retrieval of emotional memory from the hippocampus seems to protect from states of fear for aversive stimulation during the UCS free extinction phase.

4.4. Association of fMRI activation and SCR

In an earlier study we already described associations of SCR with orbitofrontal fMRI-activation during observation of emotionally relevant pictures (Anders et al., 2004). This area had also been the target for transcranial down-modulation during successful lying in a thief role play accompanied by lowered SCR (Karim et al., 2010). It is therefore thought to be strongly involved in conflicting situations usually associated with high SCR-amplitudes. Prior associations of SCR-variability participants revealed associations of amygdala fMRI-activation during the extinction phase (Couto-Ovejero et al., 2023) in a considerably larger number of participants. Although we expected associations between autonomic arousal (SCR) and BOLD, we did not see any relevant associations during both GVS and fear conditioning in our smaller sample. In general, rare significant correlations with SCR in our data might be due to habituation effects of the autonomic nervous system observed during both paradigms.

Future research directions might be investigating GVS in a placebocontrolled design to explore the interaction of GVS with fear conditioning. In addition, it will be interesting to explore representation of GVS and fear conditioning in patients with vestibular symptoms caused by circumscribed brain damage.

4.5. Limitations

This study aimed to investigate cortical and cerebellar activation sites. Therefore, measurement parameters were optimized for these regions. Differentiation of brainstem processing during both paradigms requires other imaging procedures. In addition, this study had been powered for comparisons between conditions but not for regression analyses which had been described to include >40 participants to show robust results (Yarkoni and Braver, 2010). Therefore, negative findings in association analyses might be due to an underpowered study for this purpose.

Our examined group mostly comprised university students which might restrict the generalizability of our results. Further research including groups with broader age range would be helpful.

5. Conclusion

The major finding of the current study was that GVS and fear conditioning in the same participants showed a considerable overlap of the cortical vestibular and the anxiety networks in fMRI. This was a necessary proof of the first imaging-based description of a structural and functional interaction of vestibular perception and anxiety as described

in a meta-analytic comparison (Neumann et al., 2023). In the latter analysis groups of participants were compared who had either received one or the other stimulation. In the actual study, regression analyses also revealed associations of insula fMRI-magnitude and trait anxiety during the extinction phase of fear conditioning. The current data support the functional interpretation of first, a top-down regulation of the PFC, an area that is part of both networks, on the vestibular insular cortex, and second, the involvement of the cerebellum in both networks.

Data availability

Data can be requested from the corresponding author.

CRediT authorship contribution statement

M. Lotze: Writing – review & editing, Writing – original draft, Visualization, Investigation, Funding acquisition, Formal analysis, Conceptualization. K. Klepzig: Writing – review & editing, Writing – original draft, Methodology, Formal analysis. T. Stephan: Methodology, Investigation. M. Domin: Methodology, Investigation. T. Brandt: Writing – review & editing, Supervision, Project administration, Conceptualization. M. Dieterich: Writing – review & editing, Writing – original draft, Supervision, Project administration, Funding acquisition, Conceptualization.

Declaration of competing interest

The authors have nothing to declare.

Acknowledgment

KK was funded by the German Foundation for Neurology (DSN, 80766090). MD was supported by the DSN (project 80721017) and by the Deutsche Forschungsgemeinschaft (DFG, German Research Foundation) under Germany's Excellence Strategy (Munich Cluster for Systems Neurology: EXC 2145 SyNergy).

Supplementary materials

Supplementary material associated with this article can be found, in the online version, at doi:10.1016/j.neuroimage.2025.121275.

References

- Anders, S., Lotze, M., Erb, M., Grodd, W., Birbaumer, N., 2004. Brain activity underlying emotional valence and arousal: a response-related fMRI study. Hum. Brain Mapp. 23, 200–209. https://doi.org/10.1002/hbm.20048.
- Andersson, J.L.R., Skare, S., Ashburner, J., 2003. How to correct susceptibility distortions in spin-echo echo-planar images: application to diffusion tensor imaging. Neuroimage 20, 870–888. https://doi.org/10.1016/S1053-8119(03)00336-7.
- Avants, B.B., Tustison, N.J., Song, G., Cook, P.A., Klein, A., Gee, J.C., 2011.
 A reproducible evaluation of ANTs similarity metric performance in brain image registration. Neuroimage 54, 2033–2044. https://doi.org/10.1016/j.neuroimage.2010.09.025.
- Bedini, M., Olivetti, E., Avesani, P., Baldauf, D., 2023. Accurate localization and coactivation profiles of the frontal eye field and inferior frontal junction: an ALE and MACM fMRI meta-analysis. Brain Struct. Funct. 228, 997–1017. https://doi.org/ 10.1007/s00429-023-02641-y.
- Benedek, M., Kaernbach, C., 2010. A continuous measure of phasic electrodermal activity. J. Neurosci. Methods 190, 80–91. https://doi.org/10.1016/j. ineumeth.2010.04.028.
- Best, C., Tschan, R., Eckhardt-Henn, A., Dieterich, M., 2009. Who is at risk for ongoing dizziness and psychological strain after a vestibular disorder? Neuroscience 164, 1579–1587. https://doi.org/10.1016/j.neuroscience.2009.09.034.
- Bigelow, R.T., Semenov, Y.R., du Lac, S., Hoffman, H.J., Agrawal, Y., 2016. Vestibular vertigo and comorbid cognitive and psychiatric impairment: the 2008 national health interview survey. J. Neurol. Neurosurg. Psychiatry 87, 367–372. https://doi. org/10.1136/jnnp-2015-310319.
- Brandt, T., 1996. Phobic postural vertigo. Neurology 46, 1515–1519. https://doi.org/ 10.1212/wnl.46.6.1515.

Brandt, T., Dieterich, M., 2020. 'Excess anxiety' and 'less anxiety': both depend on vestibular function. Curr. Opin. Neurol. 33, 136–141. https://doi.org/10.1097/ WCQ.000000000000771

- Brandt, T., Dieterich, M., 2019. Thalamocortical network: a core structure for integrative multimodal vestibular functions. Curr. Opin. Neurol. 32, 154–164. https://doi.org/ 10.1097/WCO.0000000000000038.
- Bzdúšková, D., Marko, M., Hirjaková, Z., Kimijanová, J., Hlavačka, F., Riečanský, I., 2022. The effects of virtual height exposure on postural control and psychophysiological stress are moderated by individual height intolerance. Front. Hum. Neurosci. 15, 773091. https://doi.org/10.3389/fnhum.2021.773091.
- Cavin, I.D., Glover, P.M., Bowtell, R.W., Gowland, P.A., 2007. Thresholds for perceiving metallic taste at high magnetic field. Magn. Reson. ImAging 26, 1357–1361. https://doi.org/10.1002/imri.21153
- Coelho, C.M., Balaban, C.D., 2015. Visuo-vestibular contributions to anxiety and fear. Neurosci. Biobehav. Rev. 48, 148–159. https://doi.org/10.1016/j. psubjects/2014.10.023
- Couto-Ovejero, S., Ye, J., Kind, P.C., Till, S.M., Watson, T.C., 2023. Cerebellar contributions to fear-based emotional processing: relevance to understanding the neural circuits involved in autism. Front. Syst. Neurosci. 17, 1229627. https://doi. org/10.3389/fnsys.2023.1229627.
- Decker, J., Limburg, K., Henningsen, P., Lahmann, C., Brandt, T., Dieterich, M., 2019. Intact vestibular function is relevant for anxiety related to vertigo. J. Neurol. 266, 89–92. https://doi.org/10.1007/s00415-019-09351-8.
- Dibbets, P., Evers, E.A.T., 2017. The influence of State anxiety on fear discrimination and extinction in females. Front. Psychol. 08. https://doi.org/10.3389/ fpsyg.2017.00347.
- Dieterich, M., Bense, S., Lutz, S., Drzezga, A., Stephan, T., Bartenstein, P., Brandt, T., 2003. Dominance for vestibular cortical function in the non-dominant hemisphere. Cereb. Cortex. 13, 994–1007. https://doi.org/10.1093/cercor/13.9.994.
- Dieterich, M., Brandt, T., 2018. The parietal lobe and the vestibular system. Handbook of Clinical Neurology. Elsevier, pp. 119–140. https://doi.org/10.1016/B978-0-444-63622-5.00006-1.
- Dieterich, M., Brandt, T., 2008. Functional brain imaging of peripheral and central vestibular disorders. Brain 131, 2538–2552. https://doi.org/10.1093/brain/awn042
- Dieterich, M., Staab, J.P., Brandt, T., 2016. Functional (psychogenic) dizziness. Handb. Clin. Neurol. 139, 447–468. https://doi.org/10.1016/B978-0-12-801772-2.00037-0.
- Dunlap, P.M., Staab, J.P., Sparto, P.J., Furman, J.M., Whitney, S.L., 2025. Psychosocial factors are associated with community mobility and participation in persons with dizziness. Front. Neurol. 16, 1531204. https://doi.org/10.3389/ fneur.2025.1531204.
- Eckhardt-Henn, A., Best, C., Bense, S., Breuer, P., Diener, G., Tschan, R., Dieterich, M., 2008. Psychiatric comorbidity in different organic vertigo syndromes. J. Neurol. 255, 420–428. https://doi.org/10.1007/s00415-008-0697-x.
- Eickhoff, S.B., Weiss, P.H., Amunts, K., Fink, G.R., Zilles, K., 2006. Identifying human parieto-insular vestibular cortex using fMRI and cytoarchitectonic mapping. Hum. Brain Mapp. 27, 611–621. https://doi.org/10.1002/hbm.20205.
- Flor, H., 2012. New developments in the understanding and management of persistent pain. Curr. Opin. Psychiatry 25, 109–113. https://doi.org/10.1097/ YCO.0b013e3283503510.
- Fullana, M.A., Albajes-Eizagirre, A., Soriano-Mas, C., Vervliet, B., Cardoner, N., Benet, O., Radua, J., Harrison, B.J., 2018. Fear extinction in the human brain: a meta-analysis of fMRI studies in healthy participants. Neurosci. Biobehav. Rev. 88, 16-25. https://doi.org/10.1016/j.neubiorev.2018.03.002.
- Gavgani, A.M., Nesbitt, K.V., Blackmore, K.L., Nalivaiko, E., 2017. Profiling subjective symptoms and autonomic changes associated with cybersickness. Auton. Neurosci. 203, 41–50. https://doi.org/10.1016/j.autneu.2016.12.004.
- Giannakakis, G., Grigoriadis, D., Giannakaki, K., Simantiraki, O., Roniotis, A., Tsiknakis, M., 2022. Review on psychological stress detection using biosignals. IEEE Trans. Affect. Comput. 13, 440–460. https://doi.org/10.1109/ TAFFC.2019.2927337.
- Gloor-Juzi, T., Kurre, A., Straumann, D., De Bruin, E.D., 2012. Translation and validation of the vertigo symptom scale into German: a cultural adaption to a wider Germanspeaking population. BMC Ear. Nose Throat. Disord. 12, 7. https://doi.org/10.1186/ 1472-6815-12-7
- Harrison, B.J., Fullana, M.A., Soriano-Mas, C., Via, E., Pujol, J., Martínez-Zalacaín, I., Tinoco-Gonzalez, D., Davey, C.G., López-Solà, M., Pérez Sola, V., Menchón, J.M., Cardoner, N., 2015. A neural mediator of human anxiety sensitivity. Hum. Brain Mapp. https://doi.org/10.1002/hbm.22889.
- Holtz, K., Pané-Farré, C.A., Wendt, J., Lotze, M., Hamm, A.O., 2012. Brain activation during anticipation of interoceptive threat. Neuroimage 61, 857–865. https://doi. org/10.1016/j.neuroimage.2012.03.019.
- Hüfner, K., Binetti, C., Hamilton, D.A., Stephan, T., Flanagin, V.L., Linn, J., Labudda, K., Markowitsch, H., Glasauer, S., Jahn, K., Strupp, M., Brandt, T., 2011. Structural and functional plasticity of the hippocampal formation in professional dancers and slackliners. Hippocampus 21, 855–865. https://doi.org/10.1002/hipo.20801.
- Indovina, I., Robbins, T.W., Núñez-Elizalde, A.O., Dunn, B.D., Bishop, S.J., 2011. Fear-conditioning mechanisms associated with trait vulnerability to anxiety in humans. Neuron 69, 563–571. https://doi.org/10.1016/j.neuron.2010.12.034.
- Karim, A.A., Schneider, M., Lotze, M., Veit, R., Sauseng, P., Braun, C., Birbaumer, N., 2010. The truth about lying: inhibition of the anterior prefrontal cortex improves deceptive behavior. Cereb. Cortex 20, 205–213. https://doi.org/10.1093/cercor/ hbp.000
- Kelly, R.M., Strick, P.L., 2003. Cerebellar loops with motor cortex and prefrontal cortex of a nonhuman primate. J. Neurosci. 23, 8432–8444. https://doi.org/10.1523/ JNEUROSCI.23-23-08432.2003.

- Laux, L., Glanzmann, P., Schaffner, P., Spielberger, C.D., 1981. Das State-Trait-Angstinventar (STAI): Theoretische Grundlagen und Handanweisung. Beltz, Weinheim
- Lahmann, C., Henningsen, P., Brandt, T., Strupp, M., Jahn, K., Dieterich, M., Eckhardt-Henn, A., Feuerecker, R., Dinkel, A., Schmid, G., 2015. Psychiatric comorbidity and psychosocial impairment among patients with vertigo and dizziness. J. Neurol. Neurosurg. Psychiatry 86, 302–308. https://doi.org/10.1136/jnnp-2014-307601.
- Lindner, K., Neubert, J., Pfannmöller, J., Lotze, M., Hamm, A.O., Wendt, J., 2015. Fear-potentiated startle processing in humans: parallel fMRI and orbicularis EMG assessment during cue conditioning and extinction. Int. J. Psychophysiol. 98, 535–545. https://doi.org/10.1016/j.ijpsycho.2015.02.025.
- Lonsdorf, T.B., Menz, M.M., Andreatta, M., Fullana, M.A., Golkar, A., Haaker, J., Heitland, I., Hermann, A., Kuhn, M., Kruse, O., Meir Drexler, S., Meulders, A., Nees, F., Pittig, A., Richter, J., Römer, S., Shiban, Y., Schmitz, A., Straube, B., Vervliet, B., Wendt, J., Baas, J.M.P., Merz, C.J., 2017. Don't fear 'fear conditioning': methodological considerations for the design and analysis of studies on human fear acquisition, extinction, and return of fear. Neurosci. Biobehav. Rev. 77, 247–285. https://doi.org/10.1016/j.neubiorev.2017.02.026.
- Lopez, C., Blanke, O., Mast, F.W., 2012. The human vestibular cortex revealed by coordinate-based activation likelihood estimation meta-analysis. Neuroscience 212, 159–179. https://doi.org/10.1016/j.neuroscience.2012.03.028.
- Lotze, M., Heymans, U., Birbaumer, N., Veit, R., Erb, M., Flor, H., Halsband, U., 2006. Differential cerebral activation during observation of expressive gestures and motor acts. Neuropsychologia 44, 1787–1795. https://doi.org/10.1016/j.neuropsychologia.2006.03.016.
- Lotze, M., Veit, R., Anders, S., Birbaumer, N., 2007. Evidence for a different role of the ventral and dorsal medial prefrontal cortex for social reactive aggression: an interactive fMRI study. Neuroimage 34, 470–478. https://doi.org/10.1016/j. neuroimage.2006.09.028.
- Lueken, U., Straube, B., Yang, Y., Hahn, T., Beesdo-Baum, K., Wittchen, H.-U., Konrad, C., Ströhle, A., Wittmann, A., Gerlach, A.L., Pfleiderer, B., Arolt, V., Kircher, T., 2015. Separating depressive comorbidity from panic disorder: a combined functional magnetic resonance imaging and machine learning approach. J. Affect. Disord. 184, 182–192. https://doi.org/10.1016/j.jad.2015.05.052.
- Lykken, D.T., Venables, P.H., 1971. Direct measurement of skin conductance: a proposal for standardization. Psychophysiology 8, 656–672. https://doi.org/10.1111/j.1469-8986.1971.tb00501.x.
- McCarthy, B., Datta, S., Sesa-Ashton, G., Wong, R., Henderson, L.A., Dawood, T., Macefield, V.G., 2023. Top-down control of vestibular inputs by the dorsolateral prefrontal cortex. Exp. Brain Res. 241, 2845–2853. https://doi.org/10.1007/ s00221-023-06722-6.
- McCarthy, B., Rim, D., Sesa-Ashton, G., Crawford, L.S., Dawood, T., Henderson, L.A., Macefield, V.G., 2025. Electrical stimulation of the dorsolateral prefrontal cortex inhibits vestibular signalling in humans: a BOLD fMRI study. Brain Stimul. 18, 627–639. https://doi.org/10.1016/j.brs.2025.02.022.
- Medina, J.F., Christopher Repa, J., Mauk, M.D., LeDoux, J.E., 2002. Parallels between cerebellum- and amygdala-dependent conditioning. Nat. Rev. Neurosci. 3, 122–131. https://doi.org/10.1038/nrn728.
- Neumann, N., Fullana, M.A., Radua, J., Brandt, T., Dieterich, M., Lotze, M., 2023. Common neural correlates of vestibular stimulation and fear learning: an fMRI meta-analysis. J. Neurol. 270, 1843–1856. https://doi.org/10.1007/s00415-023-11568-7.
- Padovan, L., Becker-Bense, S., Flanagin, V.L., Strobl, R., Limburg, K., Lahmann, C., Decker, J., Dieterich, M., 2023. Anxiety and physical impairment in patients with central vestibular disorders. J. Neurol. 270, 5589–5599. https://doi.org/10.1007/ s00415-023-11871-3
- Palm, U., Kirsch, V., Kübler, H., Sarubin, N., Keeser, D., Padberg, F., Dieterich, M., 2019. Transcranial direct current stimulation (tDCS) for treatment of phobic postural vertigo: an open label pilot study. Eur. Arch. Psychiatry Clin. Neurosci. 269, 269–272. https://doi.org/10.1007/s00406-018-0894-2.
- Raskin, M., 1975. Decreased skin conductance response habituation in chronically anxious patients. Biol. Psychol. 2, 309–319. https://doi.org/10.1016/0301-0511 (75)90039-3.

- Ren, X., White, E.J., Kuplicki, R., Paulus, M.P., Ironside, M., Aupperle, R.L., Stewart, J.L., 2025. Differential insular cortex activation during reward anticipation in major depressive disorder with and without anxiety. Biol. Psychiatry Cogn. Neurosci. NeuroimAging S2451-9022 (25), 00057. https://doi.org/10.1016/j.bpsc.2025.02.001. -6.
- Saman, Y., Mclellan, L., Mckenna, L., Dutia, M.B., Obholzer, R., Libby, G., Gleeson, M., Bamiou, D.E., 2016. State Anxiety Subjective Imbalance and Handicap in Vestibular Schwannoma. Front. Neurol. 7, 101. https://doi.org/10.3389/fneur.2016.00101.
- Schlund, M.W., Brewer, A.T., Magee, S.K., Richman, D.M., Solomon, S., Ludlum, M., Dymond, S., 2016. The tipping point: value differences and parallel dorsal-ventral frontal circuits gating human approach—avoidance behavior. Neuroimage 136, 94–105. https://doi.org/10.1016/j.neuroimage.2016.04.070.
- Sjouwerman, R., Lonsdorf, T.B., 2019. Latency of skin conductance responses across stimulus modalities. Psychophysiology 56, e13307. https://doi.org/10.1111/ psyp.13307.
- Spielberger, C.D., Gorsuch, R.L., Lushene, R.E., 1970. The State-Trait Anxiety Inventory Manual. Consulting Psychologists, Palo Alto, Cal. https://doi.org/10.1037/t06496-000.
- Staab, J.P., 2019. Psychiatric considerations in the management of dizzy patients. Adv. Otorhinolaryngol. 82, 170–179. https://doi.org/10.1159/000490286.
- Staab, J.P., Eckhardt-Henn, A., Horii, A., Jacob, R., Strupp, M., Brandt, T., Bronstein, A., 2017. Diagnostic criteria for persistent postural-perceptual dizziness (PPPD): consensus document of the committee for the classification of vestibular disorders of the Bárány society. J. Vestib. Res. 27, 191–208. https://doi.org/10.3233/VES-170622.
- Stephan, T., Deutschländer, A., Nolte, A., Schneider, E., Wiesmann, M., Brandt, T., Dieterich, M., 2005. Functional MRI of galvanic vestibular stimulation with alternating currents at different frequencies. Neuroimage 26, 721–732. https://doi. org/10.1016/j.neuroimage.2005.02.049.
- Tang, J., Gibson, S.J., 2005. A psychophysical evaluation of the relationship between trait anxiety, pain perception, and induced State anxiety. J. Pain. 6, 612–619. https://doi.org/10.1016/j.jpain.2005.03.009.
- Venables, C., 1980. Electrodermal activity, in: Techniques in Psychophysiology, 54.3. Wendt, J., Lotze, M., Weike, A.I., Hosten, N., Hamm, A.O., 2008. Brain activation and defensive response mobilization during sustained exposure to phobia-related and other affective pictures in spider phobia. Psychophysiology 45, 205–215. https://doi.org/10.1111/j.1469-8986.2007.00620.x.
- Wendt, J., Löw, A., Weymar, M., Lotze, M., Hamm, A.O., 2017. Active avoidance and attentive freezing in the face of approaching threat. Neuroimage 158, 196–204. https://doi.org/10.1016/j.neuroimage.2017.06.054.
- Wildgruber, D., Ackermann, H., Kreifelts, B., Ethofer, T., 2006. Cerebral processing of linguistic and emotional prosody: fMRI studies. Prog. Brain Res. 156, 249–268. https://doi.org/10.1016/S0079-6123(06)56013-3.
- Wong, R., Sesa-Ashton, G., Datta, S., McCarthy, B., Henderson, L.A., Dawood, T., Macefield, V.G., 2023. The role of the dorsolateral prefrontal cortex in control of skin sympathetic nerve activity in humans. Cereb. Cortex. 33, 8265–8272. https://doi. org/10.1093/cercor/bhad112.
- Yardley, L., Masson, E., Verschuur, C., Haacke, N., Luxon, L., 1992. Symptoms, anxiety and handicap in dizzy patients: development of the Vertigo symptom scale. J. Psychosom. Res. 36, 731–741. https://doi.org/10.1016/0022-3999(92)90131-K.
- Yarkoni, T., Braver, T.S., 2010. Cognitive neuroscience approaches to individual differences in working memory and executive control: conceptual and methodological issues. In: Gruszka, A., Matthews, G., Szymura, B. (Eds.), Handbook of Individual Differences in Cognition, The Springer Series on Human Exceptionality. Springer New York, New York, NY, pp. 87–107. https://doi.org/10.1007/978-1-4419-1210-7-6.
- Zhao, Y., Mei, Y., Liu, Z., Sun, J., Tian, Y., 2025. Molecularly engineered supramolecular fluorescent chemodosimeter for measuring epinephrine dynamics. Nat. Commun. 16, 1848. https://doi.org/10.1038/s41467-025-57100-5.
- zu Eulenburg, P., Caspers, S., Roski, C., Eickhoff, S.B., 2012. Meta-analytical definition and functional connectivity of the human vestibular cortex. Neuroimage 60, 162–169. https://doi.org/10.1016/j.neuroimage.2011.12.032.